NORSAR Scientific Report No. 2-2010

Semiannual Technical Summary

1 January - 30 June 2010

Frode Ringdal (ed.)

Kjeller, August 2010

6.2 Seismic Monitoring of the North Korea Nuclear Test Site Using Multi-Channel Waveform Correlation on the Matsushiro Array (MJAR) in Japan

6.2.1 Introduction

The Democratic People's Republic of Korea (DPRK) announced on 25 May 2009 that it had conducted its second nuclear test, the first one having taken place on 9 October 2006. As was the case with the first test, the second test was detected automatically, located and reported by the International Data Center (IDC) of the Comprehensive nuclear Test-Ban-Treaty Organization (CTBTO). The only primary seismic array within 1000 km of the test site which was in IDC operations at the times of both nuclear tests[1] is the Matsushiro array, MJAR, in Japan, at a distance of approximately 950 km. The location of MJAR with respect to the test site and the other IMS seismic stations in the region is displayed in Figure 6.2.1. Despite high SNR signals from both 2006 and 2009 events, MJAR failed on both occasions to report a detection with a qualitatively correct phase classification and backazimuth estimate. Because of this, although arrival time measurements at MJAR could be used to constrain the reviewed event location estimates, the array did not contribute to the fully automatic preliminary event locations. Signals at MJAR are notoriously incoherent, even at relatively low frequencies for signals from events at teleseismic distances (Kato et al., 2005). The incoherency problems are likely to be exacerbated for the more dispersed, high-frequency regional arrivals. Gibbons et al. (2008) demonstrated that, due to the relatively large array aperture, an incoherent slowness estimate for regional Pn phases may me more effective than attempting coherent f-k analysis.

The similarity between the signals from the two nuclear tests has been noted in numerous studies. In particular, the ripple-for-ripple likeness at many stations has allowed very accurate relative time measurements to be made for high-precision relative event location estimates. Wen and Long (2010), using differential time measurements from stations at regional distances, obtained a location for the 2009 test which was ~2.2 km to the west and ~0.7 km to the north of the 2006 test. Selby (2010), using an entirely distinct network of stations - a set of primary IMS seismic arrays at teleseismic distances, concluded a relative location of ~1.8 km to the west and ~0.3 km to the north, but points out that the two relative locations are consistent to within the appropriate uncertainties. While MJAR was not one of the IMS seismic arrays selected by Selby (2010), the upper panel of Figure 6.2.2 demonstrates great similarity between the two signals. In particular, we note that the similarity between the signals from the two events on a single sensor is far greater than the similarity between two signals from the same event on different sensors. This is almost surprising considering that the three channels displayed, MJA0_HHZ, MJA1_HHZ, and MJA2_HHZ, are separated by distances of 1.1 km, 1.65 km, and 1.60 km; of the same order as or less than the estimated distance between the two event epicenters.

1. The KSRS array in South Korea also recorded the first test, but was not certified until November 2006 and data from this station were not available in the operational pipeline at the IDC on October 9, 2006.

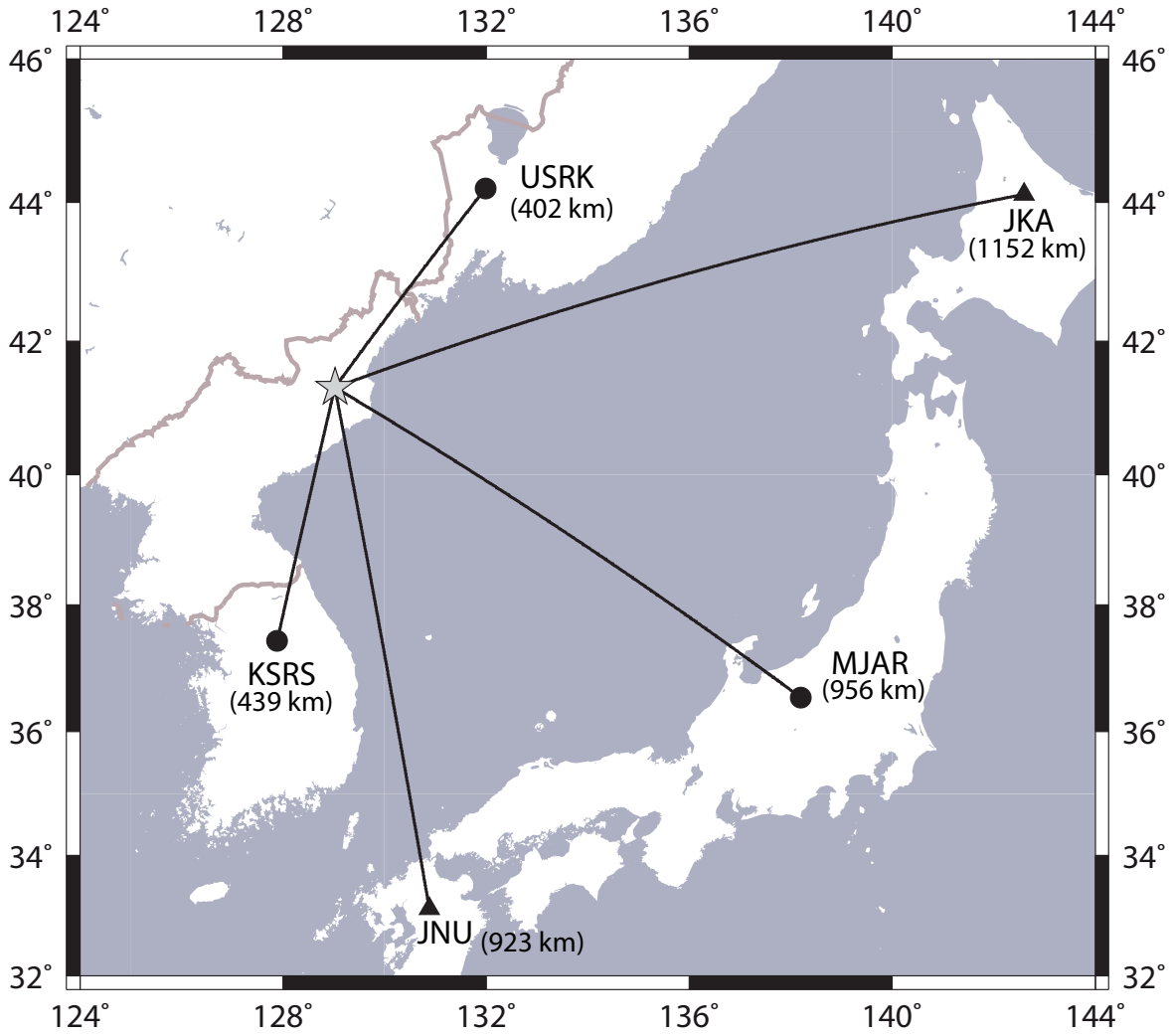

Fig. 6.2.1. Location estimate for the May 25, 2009, North Korea nuclear test with respect to the closest five IMS stations. Circles indicate primary seismic array stations and triangles indicate auxiliary 3-component stations.

The lower panel of Figure 6.2.2 indicates that the values of the correlation coefficient (or rather a related detection statistic which will be defined precisely in the next section) at the time of the optimal match are significantly greater than the background values, making the monitoring situation a candidate for a full waveform correlation detection study. This is to say that we take a signal template for the 2006 test, and correlate this with continuous MJAR data according to the formulation of Gibbons and Ringdal (2006). We need to assess a) the potential for automatically detecting subsequent nuclear tests at that site and b) monitoring the false alarm rate associated with such a detection scheme.

Spectral analysis on the MJAR signals indicate that the best frequency band is likely to be 2 - 8 Hz. In the correlation procedure described here, all waveforms are bandpass filtered in this frequency band prior to the correlation.

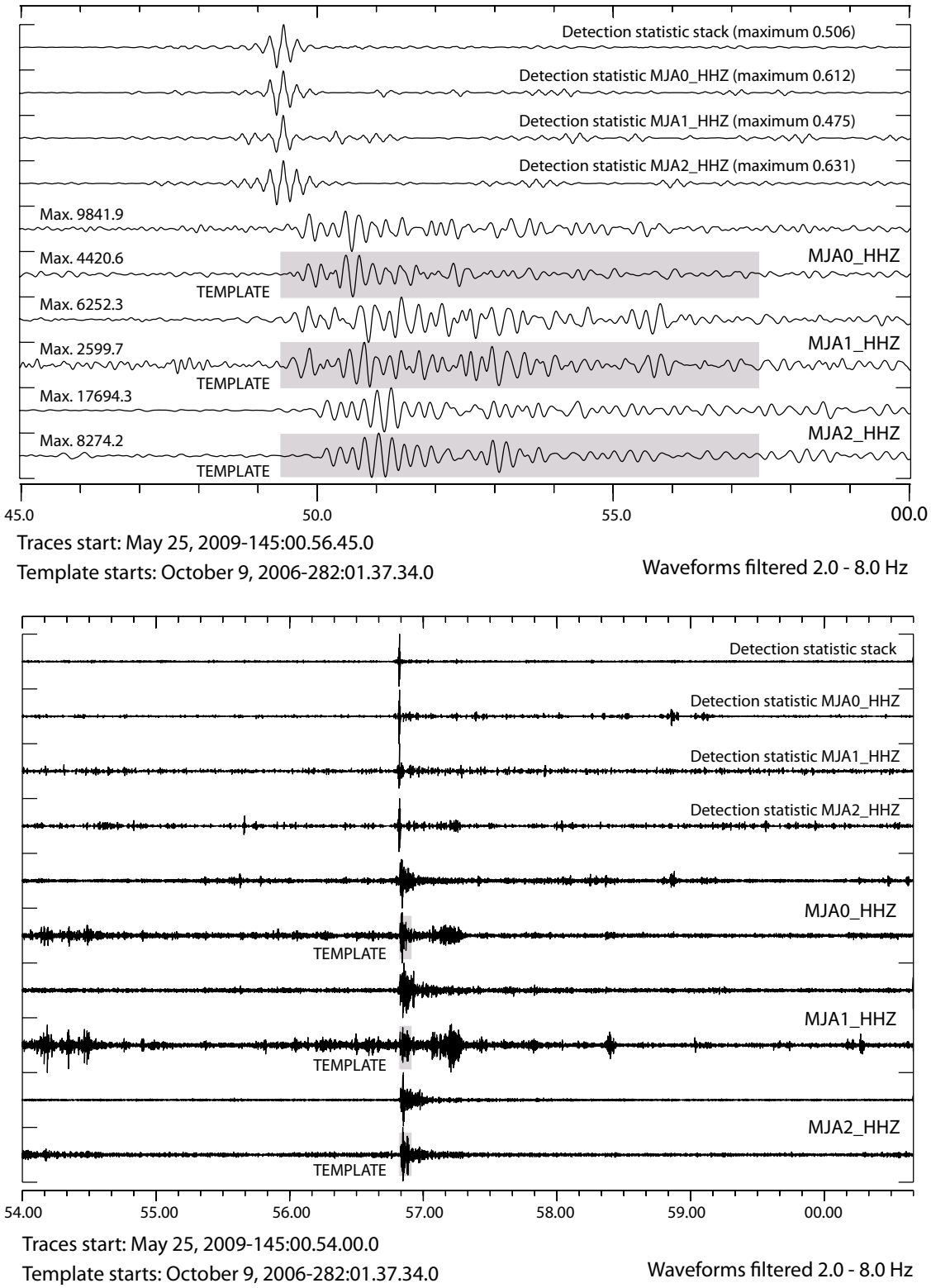

Fig. 6.2.2. Waveforms from three channels of the MJAR array from the May 25, 2009, DPRK nuclear test aligned with the corresponding waveforms from the October 9, 2006, event. The corresponding individual channel detection statistic traces are displayed together with the array stack. The upper panel is a close-up of the lower panel.

6.2.2 A Multi-Channel Correlation Detection Procedure

Formulation

The vector of ***N*** consecutive time-samples containing the waveform template recorded on sensor ***i*** is denoted x_i , where it is understood that the data is scaled a priori to give a unit norm:

$$|\boldsymbol{x}_i| = 1. \qquad (6.2.1)$$

If $y_i(t)$ denotes the vector of ***N*** consecutive time-samples starting at time ***t*** on sensor ***i*** then

$$C_i(t) = \frac{(\ \boldsymbol{x}_i.\boldsymbol{y}_i(t)\ )\,\mathrm{abs}(\ \boldsymbol{x}_i.\boldsymbol{y}_i(t)\ )}{(\ \boldsymbol{y}_i(t).\boldsymbol{y}_i(t)\ )} \qquad (6.2.2)$$

provides a signal-specific detection statistic for this single sensor indicating the degree of similarity between the unit-norm template vector and the time-series beginning at time ***t***. $C(t)$ resembles the square of the fully-normalized correlation coefficient (avoiding the computational expense of calculating the square roots for each sample) but maintains the sign such that the array detection statistic for ***M*** sensors

$$C(t) = M^{-1}\sum_{i=1}^{M} C_i(t) \qquad (6.2.3)$$

results in cancellation in the absence of alignment of features in the individual traces.

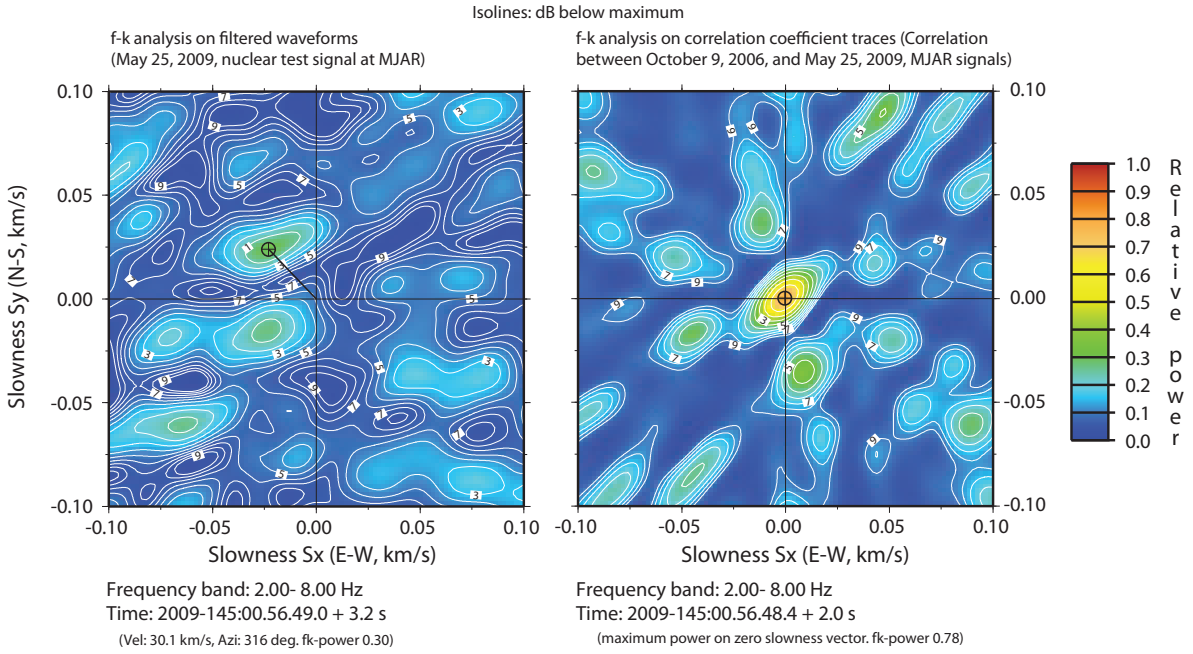

Fig. 6.2.3. Frequency-wavenumber spectrum on the MJAR array of (left) a 3.2 second long data window for Pn arrival for the May 25, 2009, test and (right) for the single channel detection statistic traces for a 2.0 second window centered at the time of the local maximum (see Fig. 6.2.2). Note that the relative power in the right hand panel is far higher than that in the left indicating that the incoming wavefront corresponds far better with the waveform template than with a plane wavefront model. The zero slowness vector in the right hand panel indicates that the incoming and template wavefronts approached the array from the same direction (Gibbons and Ringdal, 2006). Note that the slowness estimate inferred in the left panel is not consistent qualitatively with the predicted arrival from the North Korea test site.

Most importantly, given a detection on C(t), performing frequency-wavenumber or f-k analysis (e.g. Capon, 1969; Kennett, 2002) on the individual detection statistic traces, $C_i(t)$, allows any detection resulting from coincidental similarity between two wavefronts approaching from slightly different directions to be screened out automatically (Gibbons and Ringdal, 2006; see Figure 6.2.3, right hand panel). This post-processing step would not be possible had the sign information been lost, and has been demonstrated to filter out the vast majority of false alarms when detecting events from a source of repeating seismicity even when there is significant waveform dissimilarity between subsequent events (e.g. Gibbons and Ringdal, 2010).

Any detector requires a threshold which must be exceeded in order for a detection to be reported. In this study we follow an idea similar to that of Shelly et al. (2007) where triggers are identified as outliers to the distribution of the detection statistic in a given time-interval. Firstly, the statistic C(t) is evaluated over a window of continuous data, typically of length close to 20 minutes. Secondly, the extreme 1% of these values are removed and the standard deviation of the remaining values calculated. Finally, the ratio between C(t) and this standard deviation is returned and referred to here as the ‘‘***Detection statistic SNR***’’.

Results for the period January 1, 2006, to June 20, 2009.

All values of the detection statistic SNR exceeding 5.0, for which the f-k analysis also resulted in an almost-zero slowness vector, were reported. Based upon the frequency-wavenumber spectrum displayed in the right hand panel of Fig. 6.2.3, a detection was passed if the implied slowness did not exceed 0.01 s/km and if the relative power exceeded 0.20. These detections are displayed in Figure 6.2.4 as a function of time.

Table 6.2.1. Number of detections obtained between January 1, 2006, and June 20, 2009, as a function of the required detection statistic ratio.

Ratio threshold	Number of detections
14.0	2
13.0	3
12.0	3
11.0	4
10.0	7
9.0	20
8.0	88
7.0	356
6.0	1248
5.0	3632

The number of detections reported for different thresholds of this ratio are displayed in Table 6.2.1 and it is clear both here and in Figure 6.2.4 that the May 25, 2009, event was detected using correlation on MJAR data with a far higher greater value of the detection statistic than at

any other time during this period of over 3 years. With an appropriate and conservative detection threshold, the 2009 test could have been detected from the template of the 2006 test with no false alarms. However, for any kind of robust monitoring of a given source region, we need to allow for considerable waveform dissimilarity.

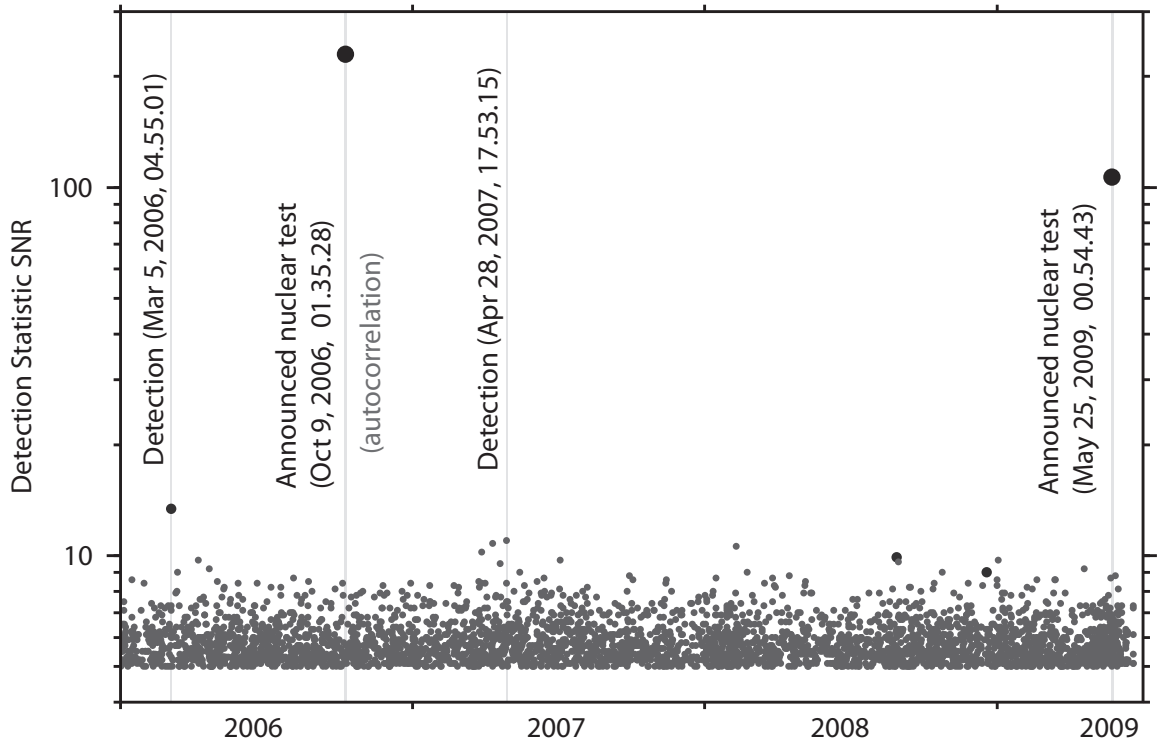

Fig. 6.2.4. Detections from the correlator on the MJAR array where the 8 second long signal template begins at a time 2006-282:01.37.32.6. The value denoted "Detection statistic SNR" is described in the text and measures the ratio between the array detection statistic C(t), defined in Equation 6.2.3, and the background level of the same quantity. Vertical bars indicate the times of the four highest values obtained in the period January 1, 2006, to June 20, 2009. The symbol size is proportional to the log of the array detection statistic.

Waveform similarity will be reduced with decreasing size of a subsequent nuclear test. This will be partly due to a decreased SNR, given a generated signal with smaller amplitude, but may also result from rather different spectral characteristics of the generated signal. There is however reason to suppose that, for this magnitude of event, within the frequency band chosen here, that there is not likely to be great variation in the signal. Gibbons et al. (2007) took a signal from a magnitude 3.5 earthquake and, using the same multi-channel procedure on the NORSAR array, successfully detected almost co-located events down to magnitude 0.5. It is likely that the greatest contribution to waveform dissimilarity will come from distance of the source location from the hypocenter of the template event.

We need in any case to set the detection threshold low enough as to allow for as great a departure as possible from the master event waveforms while keeping the false alarm rate at a minimum. Figure 6.2.4 and Table 6.2.1 provide an informative means of determining which threshold should be considered for reexamining detected signals. Selecting only the occasions where the array detection statistic exceeds the standard deviation by a factor of 10 results in only seven detections throughout the entire test period. Given the sharp increase in the number of detections at lower thresholds, 10 was determined to be a useful working SNR threshold.

6.2.3 Eliminating and Examining False Alarms

The first comment on the occurrence of false alarms is to stress the importance of the f-k post-processing. Figure 6.2.5 indicates, for intervals of the array detection statistic, the number of detections obtained both with and without the automatic screening of detections which fail to meet the requirements of the f-k post-processing algorithm. Without this waveform-alignment test, 2496 as opposed to 7 detections would have been registered over the provisional threshold SNR of 10 in the test period. This clearly constitutes a dramatic reduction in the human resources necessary to evaluate the detector output.

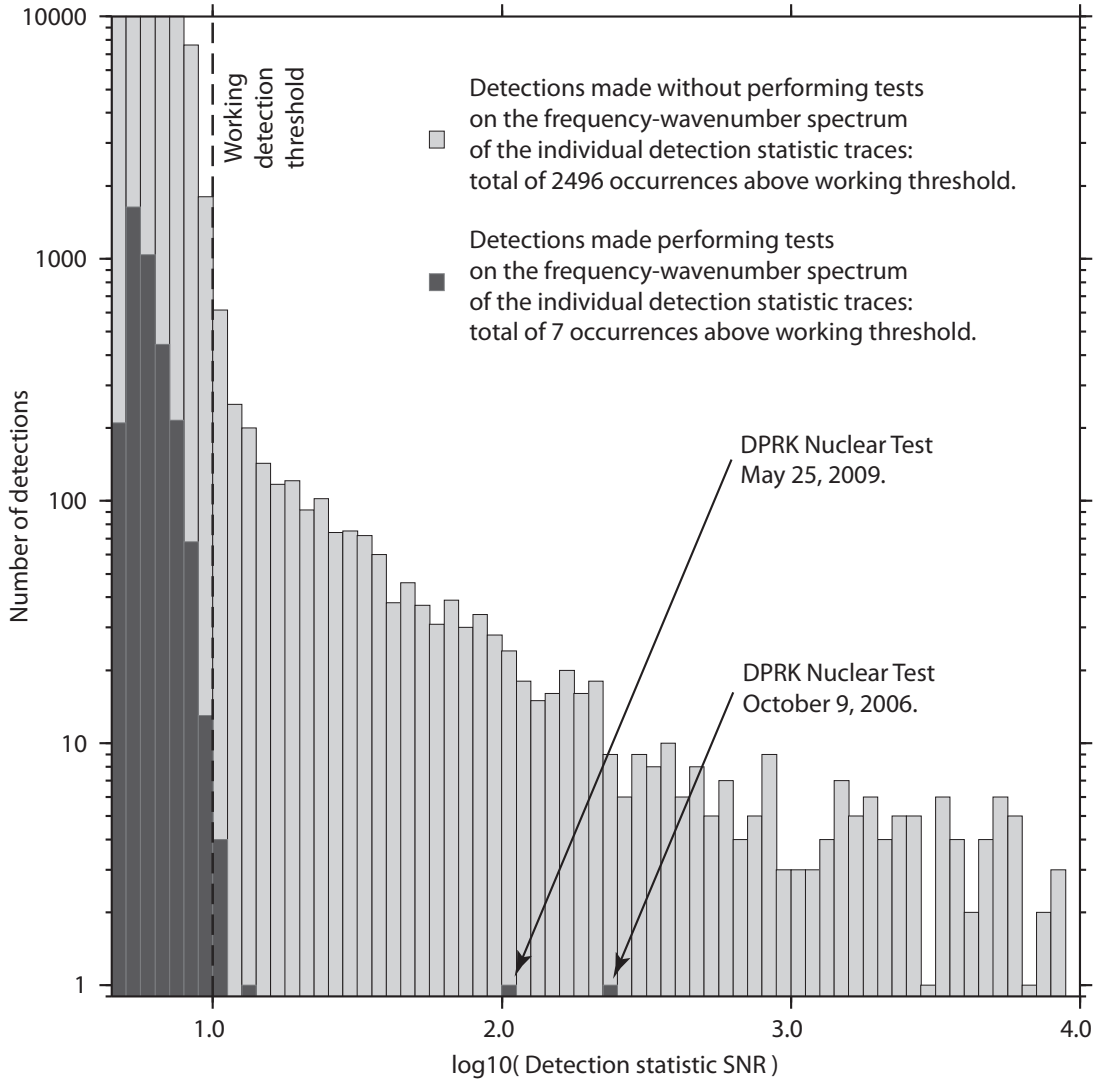

Fig. 6.2.5. Histograms of correlation detections with and without f-k post-processing on the individual channel detection statistic traces. The number of detections in each bin corresponds to the time-interval displayed in Figure 6.2.4.

Many of the detections at the lower SNR end of the spectrum are indeed caused by seismic background noise and wavefronts arriving from somewhat different directions. At the higher SNR end of the spectrum, the detections which are eliminated by the f-k post-processing are almost exclusively the result of faults in the data: e.g. gaps and spikes. A data discontinuity will frequently either affect one channel only or will affect all channels simultaneously. The multi-

channel waveform template has encoded an intrinsic time-dependence which is only likely to produce aligned correlation coefficient traces if the incoming wavefield encodes the same time-dependence. It is of course frequently possible to exclude such false alarms by other quality control methods. However, the simplicity of the f-k post-processing method, coupled with its ability to screen a full spectrum of false alarms, makes it both a robust and effective method of online, automatic quality control.

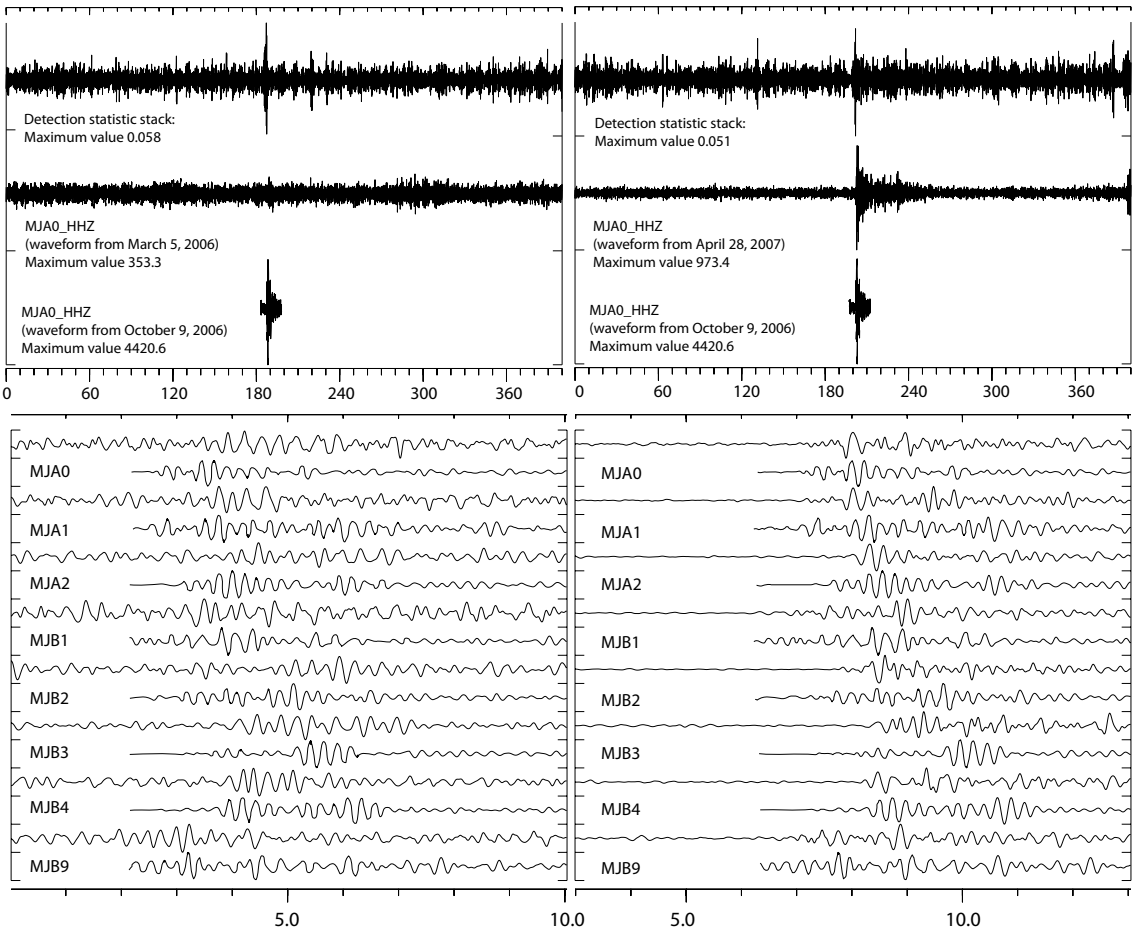

Fig. 6.2.6. Waveforms and detection statistic stack traces for the two correlation detections with the highest values of the detection statistic SNR (the announced nuclear tests excluded). In each waveform couplet, the lowermost trace is the template from the 2006 DPRK nuclear test signal.

Of the small number of detections which both exceeded the nominal detection threshold and which passed the f-k post-processing tests, the two "best" detections are displayed in Figure 6.2.6. In the right hand panel, the correlation detection clearly corresponds to a phase arrival which can be associated with an event in the bulletin of the International Seismological Center (ISC, http://www.isc.ac.uk/) with origin time, latitude and longitude 2007-118:17.54.52.3, 37.45 degrees N, 136.46 degrees E. The location of this event is shown in the map in Figure 6.2.7 and clearly falls almost on the great circle path to the North Korea test site. The implication of this is that while the source type and location of the events were very different, the fact that the resulting wavefront has propagated through the rock close to the array in almost the same direction as the wavefront from the nuclear test, both the correlation and the alignment of waveforms was sufficiently good to result in a detection.

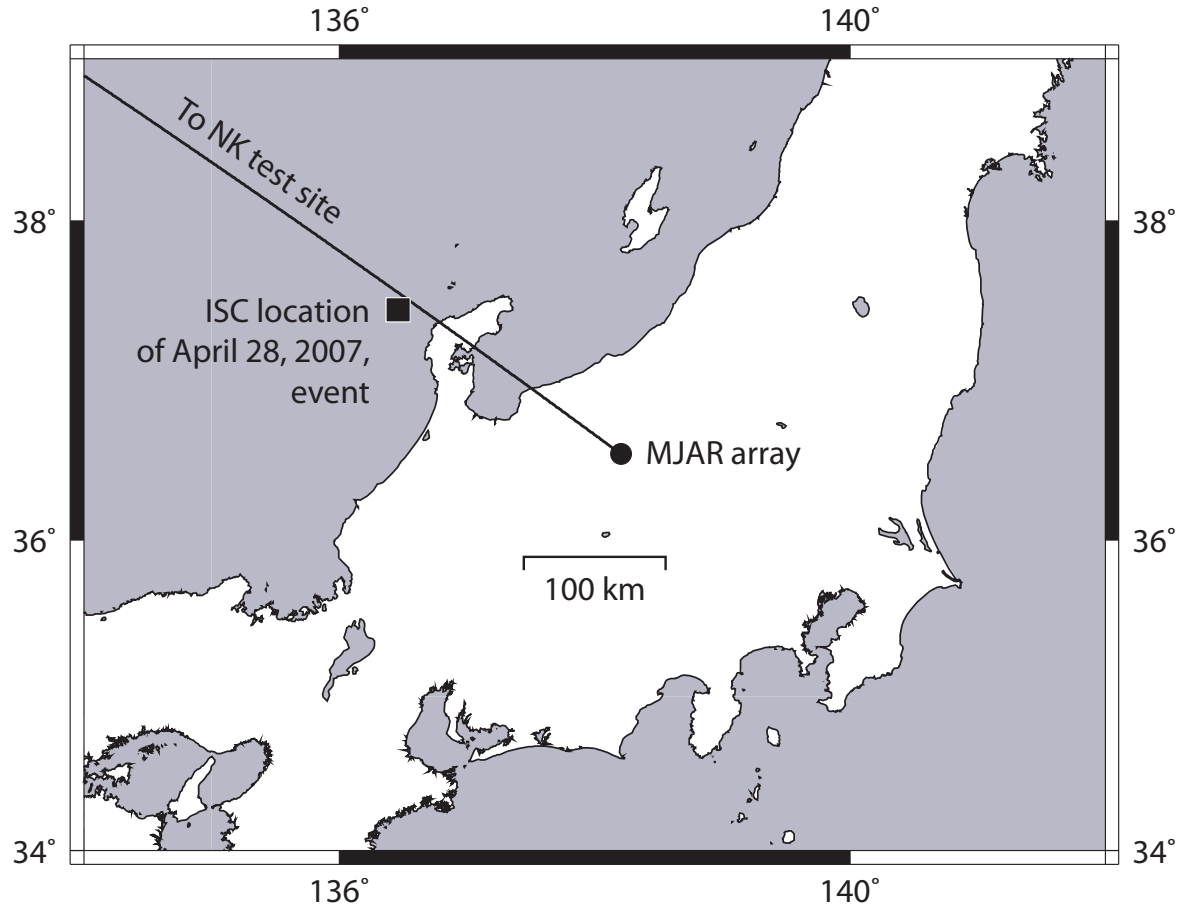

Fig. 6.2.7. ISC location of the April 28, 2007, event relative to the MJAR array.

The detection displayed in the left hand panel of Figure 6.2.6 does not appear to result from a visible signal, and no event is present in the ISC bulletin which could have generated a signal at this time and place. The segment of data which correlates best with the template starting at time 2006-282:01.37.34.0 begins at a time 2006-064:04.57.07.4. Data from the INCN and MDJ stations were obtained from the IRIS DMC for this time period and no evidence was observed in these waveforms for an event close to the test-site.

6.2.4 Examining the Detection Threshold

It is of great interest to examine how effective the correlation procedure is at detecting copies of the signals from the two announced nuclear tests, scaled down and submerged into background noise on the MJAR array. The experiment is designed to examine the magnitudes down to which events will be detected reliably using the correlation procedure. No spectral rescaling is applied to the data; we defend a linear scaling of filtered waveforms by referring to the results of Gibbons et al. (2007). Two different experiments were carried out. In the first, copies of the signal from the 2006 test were scaled down into background noise and, in the second, copies of the signal from the 2009 test were used. In all cases, the waveform template used for the matched filter was the signal from the 2006 test. Both experiments were essentially a repeat of the standard detection run described above, except that for every 20 minute long segment of data, a scaling factor between 0.0001 and 1.0 was selected (pseudo-randomly) and a copy of

the signal of interest was submerged into the data with this scaling. The results of this study are displayed in Figure 6.2.8, where the scaling factor applied has been converted to an indication of the inferred event magnitude as shown.

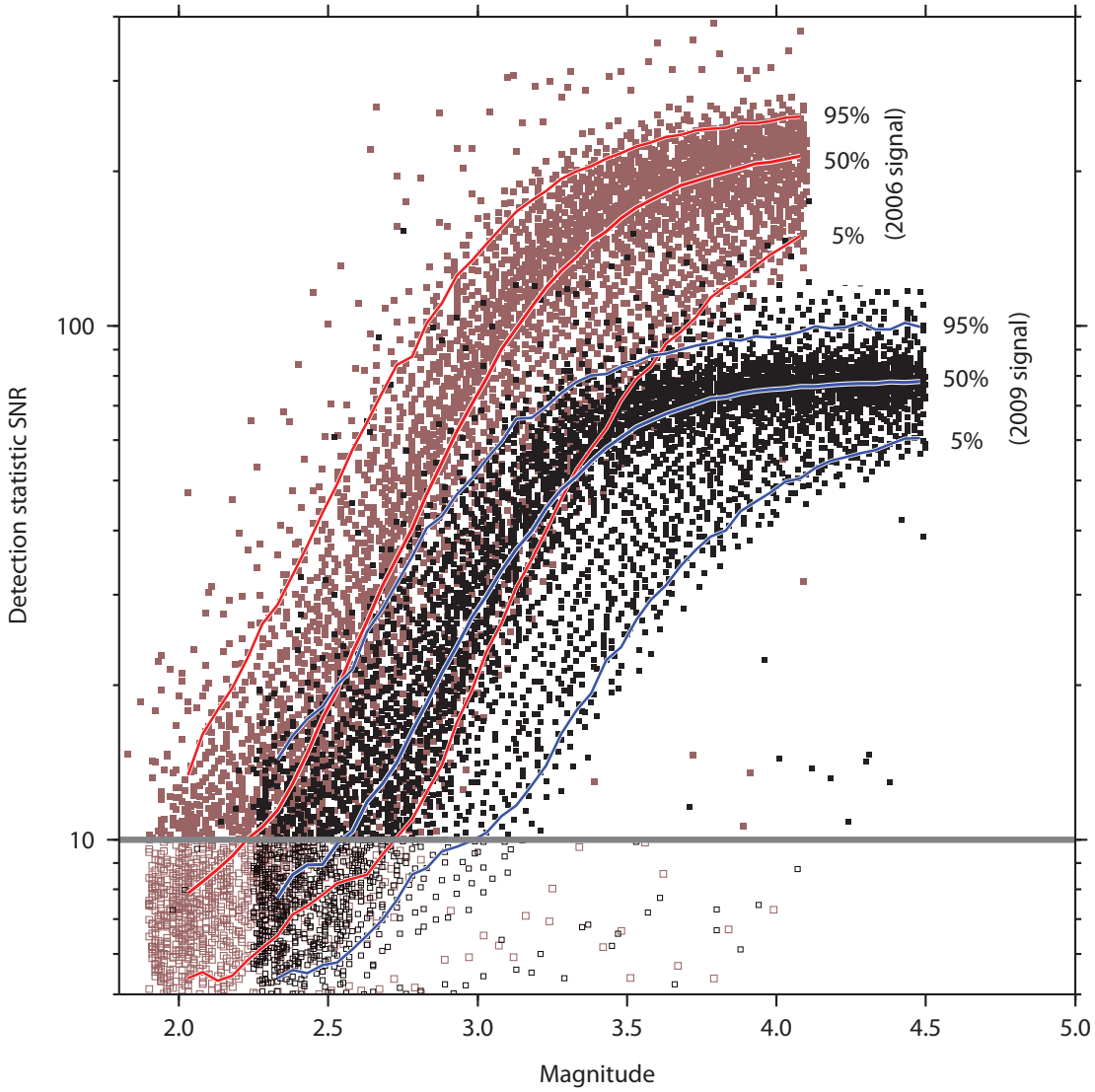

Fig. 6.2.8. Detectability using a multi-channel correlator on the MJAR array of signals from the 2006 and 2009 explosions, scaled down into different segments of background noise, using the signal from the 2006 explosion as a template. The mb magnitudes for the 2006 and 2009 events are assumed to be 4.1 and 4.5 respectively and the magnitude of the simulated events are taken to be 4.1 + log10(epsilon) and 4.5 + log10(epsilon) where epsilon is the factor that the explosion signal is scaled by before adding to the background noise at a given time. Only one in 50 of the points used to estimate the detectability curves is plotted on the graph. The detectability curves are based on the points contained in intervals of 0.05 magnitude units.

Figure 6.2.8 displays the detection statistic SNR, of which there is clearly a large spread for any given scaling factor. The time-period explored lasts from January 1, 2006, to June 20, 2009, and - considering that one submerged signal was added to the data every 20 minutes during this period - we cover every eventuality of background noise level, including the codas of large earthquakes.

The detection statistic SNR for the scaled-down copies of the 2006 signal decrease almost immediately as the magnitudes of the simulated events decrease. The values of the detection statistic SNR for the scaled down copies of the 2009 signal start at a lower level than for the 2006 signal (since the signals do have a slightly different form to the detection template) but are not affected greatly by applying a scaling factor between 0.1 and 1.0 (probably due to the large SNR of the 2009 signal). Down to a simulated magnitude of ~2.7, 95% of the submerged 2006-signals are still recording values of the detection statistic SNR above the nominal threshold of 10.0. The same is true for simulated copies of the 2009 event down to magnitudes of ~3.0. 50% of the 2009 signals scaled down to magnitude ~2.6 are being detected as are 50% of the 2006 signals scaled down to magnitude ~2.3.

6.2.5 Summary

We have demonstrated that performing multi-channel cross-correlation on the MJAR array in Japan, with a signal template taken from the October 9, 2006, North Korea nuclear test, is able to detect the signals from the May 25, 2009, North Korea test with a very low false alarm rate. Crucial to the low false alarm rate in this study is the performing of f-k analysis on the individual sensor detection statistic traces which eliminates false alarms both due to unrelated seismic signals and problems in the data.

A scaling study, whereby signals from both 2006 and 2009 tests are scaled down and submerged into the background noise, suggests that, at a detection threshold which results in a negligible number of detections, events down to magnitude ~3.0 at the site of the 2009 test are detected by the correlation procedure in 95% of cases.

It is pointed out that this study used only data from the MJAR array (Matsushiro, Japan) which, due to problems of signal incoherence at high frequencies, was unable to contribute to the automatic event location estimate for either 2006 or 2009 DPRK nuclear tests. The multi-channel correlation procedure demonstrated here is insensitive to waveform incoherence between sensors and can be used to detect signals from new events if we have a template signal from an event close-by. This is the case for the DPRK test site and many other sources of both natural and anthropogenic seismicity. Large scale correlation detectors in operational pipelines are to be advocated for automatic signal detection and event classification.

Acknowledgements

Data from the MJAR array was obtained via the IDC in Vienna, Austria.
Data from the MDJ station was obtained via the IRIS DMC and is made available via the IC network. Data from the INCN station was obtained via the IRIS DMC and is made available via the IU network.

All maps were generated using GMT software (Wessel and Smith, 1995).

References

Capon, J. (1969). High-Resolution Frequency-Wavenumber Spectrum Analysis, *Proc. IEEE*, **57**, 1408-1418.

Gibbons, S. J. and Ringdal, F. (2006). The detection of low magnitude seismic events using array-based waveform correlation, *Geophys. J. Inter.*, **165**, 149-166.

Gibbons, S. J., Ringdal, F., and Kværna, T. (2008). Detection and Characterization of Seismic Phases Using Continuous Spectral Estimation on Incoherent and Partially Coherent Arrays, *Geophys. J. Inter.*, **172**, 405-421.

Gibbons, S. J., Bøttger-Sørensen, M., Harris, D. B., and Ringdal, F. (2007). The detection and location of low magnitude earthquakes in northern Norway using multi-channel waveform correlation at regional distances, *Phys. Earth Planet. Inter.*, **160**, 285-309.

Gibbons, S. J. and Ringdal, F. (2010). Detection and Analysis of Near-Surface Explosions on the Kola Peninsula, *Pure Appl. Geophys.*, **167**, 413-436.

Kato, M., Nakanishi, I., and Takayama, H. (2005). Variation of teleseismic short-period waveforms at Matsushiro Seismic Array System, *Earth, Planets, Space*, **57**, 563-570.

Kennett, B. L. N. (2002). *The Seismic Wavefield. Volume II: Interpretation of Seismograms on Regional and Global Scales*, Cambridge University Press, Cambridge, UK. ISBN 0 521 00665 1.

Kværna, T., Ringdal, F., and Baadshaug, U. (2007). North Korea's Nuclear Test: The Capability for Seismic Monitoring of the North Korean Test Site, *Seism. Res. Lett.*, **78**, 487-497.

Selby, N. D. (2010). Relative locations of the October 2006 and May 2009 DPRK announced nuclear tests using International Monitoring System seismic arrays, *Bull. Seism. Soc. Am.*, **100**, 1779-1784.

Shelly, D. P., Beroza, G. C., and Ide, S. (2007). Non-volcanic tremor and low-frequency earthquake swarms, *Nature*, **446**, 305-307.

Wen, L., and Long, H. (2010). High-precision Location of North Korea's 2009 Nuclear Test, *Seism. Res. Lett.*, **81**, 26-29.

Wessel, P. and Smith, W. H. F. (1995). New version of the Generic Mapping Tools, *EOS Transactions of the American Geophysical Union*, **76**, 329.

S. J. Gibbons